# Void Growth and Local Necking in Biaxially Stretched Sheets

**A. NEEDLEMAN**

Assistant Professor of Engineering,
Division of Engineering,
Brown University,
Providence, R. I.
Mem. ASME

**N. TRIANTAFYLLIDIS**

Graduate Research Assistant,
Division of Engineering,
Brown University,
Providence, R.I.

*The role of void growth in triggering local necking in biaxially stretched sheets is investigated. A recently proposed constitutive equation for porous plastic materials is employed in conjunction with the model of localized necking introduced by Marciniak and Kuczynski. An increased initial volume concentration of voids within the incipient neck plays the role of the imperfection. The predictions of this analysis are compared with corresponding predictions based on classical plasticity theory with various types of initial inhomogeneities. It is found that the porous plastic material model predicts forming limit diagrams qualitatively in accord with experimental results. However, the results also show that any microstructural inhomogeneity that gives rise to a continually decreasing rate of hardening in the neck would be expected to predict qualitatively similar forming limit diagrams. It is also found that the hypothesis of an equivalent thickness imperfection is not necessarily appropriate for high hardening materials.*

## 1 Introduction

When an initially uniform sheet subject to biaxial tension is analyzed by means of the classical theory of a rigid plastic solid, local necking is not predicted to occur, [1].[1] However, practical experience [2–4] and experimental tests [5–8] clearly show that sheets subject to biaxial tension do fail by a process of localized necking. Marciniak and Kuczynski [9] demonstrated that the occurrence of localized necking could be accommodated within the framework of classical plasticity theory (smooth yield surface, normality) by postulating the presence of an initial inhomogeneity in the sheet. This inhomogeneity was taken to be in the form of a localized thickness reduction and to lie perpendicular to the major principal strain direction. In this theory local necking is instigated by a drift of the strain state in the neck toward plane strain while the remainder of the sheet undergoes proportional loading.

Azrin and Backofen [5] carried out experiments aimed at testing this Marciniak-Kuczynski, (M-K), model of localized necking. The experiments did show the drift of the strain state in the neck toward plane strain, but the magnitude of the assumed initial thickness reductions required to fit the theoretical predictions to the experimental data were much larger than those actually measured in the test specimens. Furthermore, for most of the materials tested, the dependence of the limit strain, the imposed strain at the onset of localized necking, on the imposed strain ratio was qualitatively different from that predicted by the M-K model.

As was stated by Marciniak and Kuczynski [9] and emphasized by Sowerby and Duncan [10], the thickness imperfection was intended to be regarded as a representative measure of the inhomogeneity of the material rather than as a literal thickness reduction. In order to account for the experimental results, Azrin and Backofen [5] suggested that this measure of the initial inhomogeneity would also need to depend on the imposed strain ratio. A number of more recent theoretical studies employing the basic M-K model have been carried out, e.g. [11–13], but only in [13] was an actual difference in material properties considered and in that study attention was confined to the case of equal biaxial tension.

A different line of attack was initiated by Stören and Rice [14] who showed that a simple model of a material with a vertex on its yield surface, namely a finite strain version of the simplest deformation theory of plasticity, does predict a bifurcation corresponding to the onset of local necking. In the analysis of Stören and Rice [14] the local neck is found to lie perpendicular to the major principal strain direction when the sheet is subject to biaxial tension, as is observed experimentally. The limit strains given by this analysis for biaxial tension are qualitatively more in accord with the observed dependence on imposed strain ratio than those given by the M-K analysis.

In this paper, we explicitly consider the effects of variations in material properties in conjunction with the basic M-K model of localized necking. The aim of this analysis is to determine whether or not an actual difference in material properties can account for the qualitative dependence of the limit strain on the imposed strain ratio. Particular attention is focused on the role played by void growth in triggering local necking. A constitutive relation proposed by Gurson [15, 16] for porous plastic

[1]Numbers in brackets designate References at end of paper.

Contributed by the Materials Division for publication in the JOURNAL OF ENGINEERING MATERIALS AND TECHNOLOGY. Manuscript received by the Materials Division June 22, 1977.

materials is employed. Recently, this constitutive model has been employed by Yamamoto [17] in a study of shear band formation in porous plastic materials, using a three dimensional generalization of the M-K analysis due to Rice [18]. As in [17], an increased initial void concentration inside the incipient neck plays the role of the initial inhomogeneity. Although the constitutive equation employed here is not a precise model for materials with a random initial void concentration, it is analytically convenient and permits a preliminary evaluation of the effect of void growth on localized necking. Additionally, we consider the effects of inhomogeneities in the form of differences of material properties (strain hardening exponent and yield stress) within the context of the classical plasticity theory and compare these predictions for the onset of localized necking with those of the porous material model.

## 2 Local Necking Analysis

As in the original analysis of Marciniak and Kuczynski [9], we consider an inhomogeneous band, region B in Fig. 1, in an otherwise homogeneous sheet. It is assumed that outside the band, region A in Fig. 1, homogeneous and proportional straining is maintained. Plane stress conditions are assumed to prevail both inside and outside the band.

Compatibility across the band requires,

$$\epsilon_2{}^B = \epsilon_2{}^A \tag{1}$$

where $\epsilon_2$ is the logarithmic strain parallel to the band. Here, and subsequently, the superscripts $(\ )^A$ and $(\ )^B$ refer to quantities outside and inside the band, respectively.

Equilibrium across the band is expressed by,

$$\sigma_1{}^B t^B = \sigma_1{}^A t^A \tag{2}$$

Here, $\sigma_1$ is the principal value of the Cauchy or true stress normal to the band and $t$ denotes the current thickness.

The sheet material is characterized by an elastic-plastic constitutive law relating increments of Cauchy stress to logarithmic strain of the form,

$$\dot{\sigma}_\alpha = L_{\alpha\beta}\dot{\epsilon}_\beta \tag{3}$$

where $L_{\alpha\beta}$ are the plane stress moduli and here posess the symmetry $L_{\alpha\beta} = L_{\beta\alpha}$. In this paper the summation convention is employed with Greek indices ranging from 1 to 2 and Latin indices from 1 to 3. The subscript 1 denotes principal values normal to the band, the subscript 2 denotes principal values parallel to the band, and the subscript 3 denotes principal values normal to the plane of the sheet.

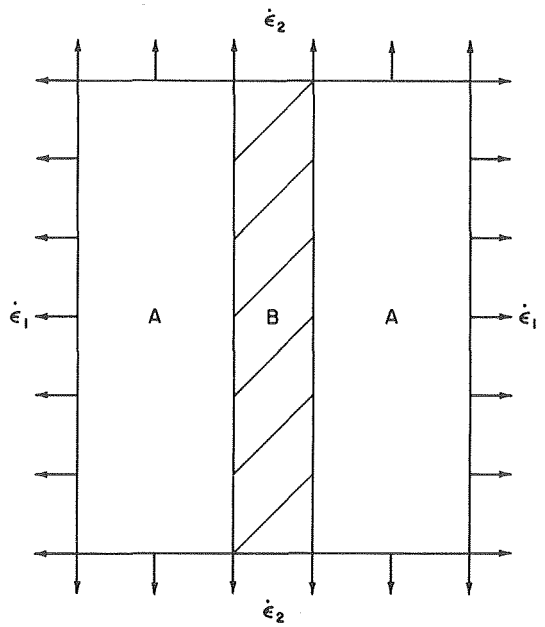


**Fig. 1 Schematic drawing of a sheet subject to biaxial tension. Region B is the local neck.**

The principal difference between the analysis given here and the original M-K analysis [9] is that by considering elastic-plastic materials the stress increments can be directly related to the strain increments by (3). For a rigid-plastic material (3) does not hold and a somewhat different formulation is required.

Taking increments in (2) and employing (3) yields,

$$t^B[L_{1\alpha}{}^B\dot{\epsilon}_\alpha{}^B + \sigma_1{}^B\dot{t}^B/t^B] = t^A[L_{1\alpha}{}^A\dot{\epsilon}_\alpha{}^A + \sigma_1{}^A\dot{t}^A/t^A] \tag{4}$$

The through-the-thickness strain increment, $\dot{\epsilon}_3$, can be related to the in-plane strain increments in the form,

$$\dot{\epsilon}_3 = \dot{t}/t = \gamma_\alpha\dot{\epsilon}_\alpha \tag{5}$$

For an incompressible material $\gamma_1 = \gamma_2 = -1$. However, due to void growth the materials considered here can exhibit plastic dilation.

Employing (5) and (1) in (4) gives,

$$(L_{11}{}^B + \sigma_1{}^B\gamma_1{}^B)\frac{d\epsilon_1{}^B}{d\epsilon_1{}^A} = \left(\frac{t^A}{t^B}\right)(L_{11}{}^A + \sigma_1{}^A\gamma_1{}^A) + \left(\frac{t^A}{t^B}\right)(L_{12}{}^A + \sigma_1{}^A\gamma_2{}^A)\rho - (L_{12}{}^B + \sigma_1{}^B\gamma_2{}^B)\rho \tag{6}$$

where $\rho$, the imposed strain ratio, is defined by,

$$\rho = \frac{d\epsilon_2{}^A}{d\epsilon_1{}^A} = \frac{\epsilon_2{}^A}{\epsilon_1{}^A} \tag{7}$$

since proportional straining is assumed to occur outside the band.

From (6) it follows that,

$$\frac{d\epsilon_1{}^B}{d\epsilon_1{}^A} \to \infty$$

when,

$$L_{11}{}^B + \sigma_1{}^B\gamma_1{}^B = 0 \tag{8}$$

Thus, local necking takes place when (8) is satisfied.

## 3 A Constitutive Relation for Porous Elastic-Plastic Materials

The constitutive relation employed in this study is one proposed by Gurson [15, 16]. In order to simplify the treatment of large strain effects, the constitutive equation will be formulated for the special case of fixed principal directions, which is all that is needed in this analysis. Based on an analysis of a single spherical void in a spherical cell, Gurson [15, 16] proposed the following approximate form for the yield surface of a randomly voided material

$$\phi = \frac{\sigma_e{}^2}{Y_m^2} + 2f\cosh\left(\frac{\sigma_1 + \sigma_2 + \sigma_3}{2Y_m}\right) - f^2 - 1 = 0 \tag{9}$$

Here, $f$ is the current volume fraction of voids, $Y_m$ is the flow stress of the matrix material, $\sigma_i$ are the principal values of the Cauchy stress acting on an element of the aggregate and $\sigma_e{}^2$ is given by

$$\sigma_e{}^2 = \sigma_1{}^2 + \sigma_2{}^2 + \sigma_3{}^2 - \sigma_1\sigma_2 - \sigma_1\sigma_3 - \sigma_2\sigma_3 \tag{10}$$

When $f = 0$, (9) reduces to the von Mises yield surface.

The increment of plastic work is given by [15],

$$\sigma_i\dot{\epsilon}_i{}^P = (1 - f)Y_m\dot{\epsilon}_m{}^P \tag{11}$$

Here $(1 - f)$ is the volume fraction of matrix material and

$\dot{\epsilon}_m{}^P$ is the increment of equivalent plastic strain in the matrix and is given in terms of the increment of flow stress in the matrix $\dot{Y}_m$ by

$$\dot{\epsilon}_m{}^P = \left(\frac{1}{E_t} - \frac{1}{\mathrm{E}}\right)\dot{Y}_m \tag{12}$$

where E is the Young's modulus of the matrix material and $E_t$ is the tangent modulus of the matrix material, which is the slope of the uniaxial true stress-natural strain curve.

Thus, (11) and (12) give

$$\dot{Y}_m = \frac{E_t\mathrm{E}}{(\mathrm{E} - E_t)Y_m}\frac{\sigma_i\dot{\epsilon}_i{}^P}{(1-f)} \tag{13}$$

Here, it will be assumed that the uniaxial stress-strain curve of the matrix material is characterized by a piecewise power law of the form

$$\epsilon_u = \begin{cases} \dfrac{\sigma_u}{\mathrm{E}} & \sigma_u < \sigma_y \\ \dfrac{\sigma_y}{\mathrm{E}}\left(\dfrac{\sigma_u}{\sigma_y}\right)^n & \sigma_u \geq \sigma_y \end{cases} \tag{14}$$

where $\epsilon_u$ and $\sigma_u$ are, respectively, the logarithmic strain and true stress in a uniaxial tension test of the matrix material.

Thus,

$$E_t = \frac{\mathrm{E}}{n}\left(\frac{Y_m}{\sigma_y}\right)^{1-n} \tag{15}$$

As shown in [15, 16], the rate of change of void volume fraction, $f$, and the plastic dilation are related by

$$\dot{f} = (1-f)(\dot{\epsilon}_1{}^P + \dot{\epsilon}_2{}^P + \dot{\epsilon}_3{}^P) \tag{16}$$

As Berg [19] and Gurson [15, 16] have noted, drawing on the argument employed by Bishop and Hill [20], plastic normality for the matrix material implies plastic normality for the matrix-void aggregate.

Thus,

$$\dot{\epsilon}_i{}^P = \Lambda\frac{\partial\phi}{\partial\sigma_i} \tag{17}$$

During plastic loading $\phi = 0$, since the current loading point must remain on the yield surface. Thus, the total rate of change of $\phi$ must be zero during plastic loading. Employing (17) in conjunction with this consistancy condition yields [15],

$$\Lambda = \frac{1}{h}\frac{\partial\phi}{\partial\sigma_i}\dot{\sigma}_i \tag{18}$$

$$h = -\left[\frac{\partial\phi}{\partial Y_m}\frac{E_t\mathrm{E}}{\mathrm{E}-E_t}\frac{\sigma_i}{(1-f)Y_m}\frac{\partial\phi}{\partial\sigma_i} + (1-f)\frac{\partial\phi}{\partial f}\left(\frac{\partial\phi}{\partial\sigma_1} + \frac{\partial\phi}{\partial\sigma_2} + \frac{\partial\phi}{\partial\sigma_3}\right)\right] \tag{19}$$

Assuming that the strain increment can be written as the sum of the elastic strain increment and the plastic strain increment, the incremental stress-strain relation is given by

$$\dot{\sigma}_i = E_{ij}(\dot{\epsilon}_j - \dot{\epsilon}_j{}^P) \tag{20}$$

where $E_{ij}$ is the matrix of elastic moduli given in terms of Young's modulus, E, and Poisson's ratio, $\nu$, by,

$$E_{ij} = \begin{cases} \dfrac{\mathrm{E}}{1+\nu} + \dfrac{\nu\mathrm{E}}{(1+\nu)(1-2\nu)} & i = j \\ \dfrac{\nu\mathrm{E}}{(1+\nu)(1-2\nu)} & i \neq j \end{cases} \tag{21}$$

Employing (17) and (18) in (20) yields the stress increment-strain increment relation for plastic loading,

$$\dot{\sigma}_i = C_{ij}\dot{\epsilon}_j \tag{22}$$

where

$$C_{ij} = E_{ij} - \frac{1}{q}E_{ik}\frac{\partial\phi}{\partial\sigma_k}E_{lj}\frac{\partial\phi}{\partial\sigma_l} \quad q = h + \frac{\partial\phi}{\partial\sigma_i}E_{ij}\frac{\partial\phi}{\partial\sigma_j} \tag{23}$$

The plastic loading condition is,

$$\frac{\partial\phi}{\partial\sigma_i}\dot{\sigma}_i > 0 \tag{24}$$

In this analysis, it is expected that the plastic loading condition (24) will be satisfied both inside and outside the neck, once initial yielding has occurred, up to the onset of localized necking. In the numerical calculations this was checked and, as expected, (24) was always satisfied once initial yielding occurred.

To obtain the plane stress moduli, the three dimensional moduli were evaluated with $\sigma_3$ set zero *after* all necessary derivatives of $\phi$ were evaluated. Then, from $\dot{\sigma}_3 = 0$, the relation (5) between the in-plane and through the thickness strains is obtained, namely

$$\gamma_\alpha = -C_{3\alpha}/C_{33} \tag{25}$$

and the plane stress moduli $L_{\alpha\beta}$ in (3) are given by,

$$L_{\alpha\beta} = C_{\alpha\beta} - \frac{C_{\alpha 3}C_{3\beta}}{C_{33}} \tag{26}$$

## 4 Results and Discussion

A numerical solution to (6) was obtained by a straightforward incremental procedure. When (8) was satisfied the calculation was terminated and the values of $\epsilon_1{}^A$ and $\epsilon_2{}^A$ at which this occurred are denoted by $\epsilon_1{}^*$ and $\epsilon_2{}^*$, respectively, and referred to as the limit strains. In all the examples considered here the parameter values $\nu^A = \nu^B = 0.3$ and $\sigma_y{}^A/E^A = 0.002$ were employed. Limit strains were calculated for $\rho = 0.1, 0.2, 0.4, 0.6, 0.8, 1.0$ and a smooth curve was drawn through these points. To facilitate accurate extrapolation to $\rho = 0$, additional limit strains were obtained for $\rho = 0.02$ and $\rho = 0.05$, in certain cases. During the computations the increment size was adjusted so that equilibrium (2) and the yield condition (9), both inside and outside the neck, were satisfied to within a tolerance of $3 \times 10^{-3}$. In many of the computations, (2) and (9) were actually satisfied to within a much smaller tolerance. To start a computation, the initial conditions inside and outside the neck were given. Namely, the values of initial thickness ratio $(t^A/t^B)_0$, the strain hardening exponents $n^A$ and $n^B$, the yield strain in the neck, $\sigma_y{}^B/E^B$, and the initial void concentrations $f_0{}^A$ and $f_0{}^B$ were specified.

Figs. 2 and 3 display forming limit curves, that is curves of the dependence of the limit strains on the imposed strain ratio, $\rho$, for the case where there is only an initial difference in initial void concentration between the material inside the neck and that outside, i.e.,

$$(t^A/t^B)_0 = 1, \quad \sigma_y{}^B/E^B = \sigma_y{}^A/E^A, \quad n^A = n^B = n \tag{27}$$

The strain hardening exponents in Figs. 2 and 3 were chosen to cover the range of strain hardening exponents exhibited by the materials employed in the experiments of [5, 6]. The aluminum tested in [6] had $n \simeq 25$ (the strain hardening exponent employed here is the reciprocal of the one used in [5, 6]), while the 301 stainless steel and the 70/30 brass used in [5] had a strain hardening exponent in the range of 1.5. A strain hardening exponent of 2.5 is representative of the value for copper and $n \simeq 4$ is a representative value for A-K steel. With the exception of the A-K steel, none of these materials seemed to exhibit a pure power law uniaxial stress strain curve so that the above identification

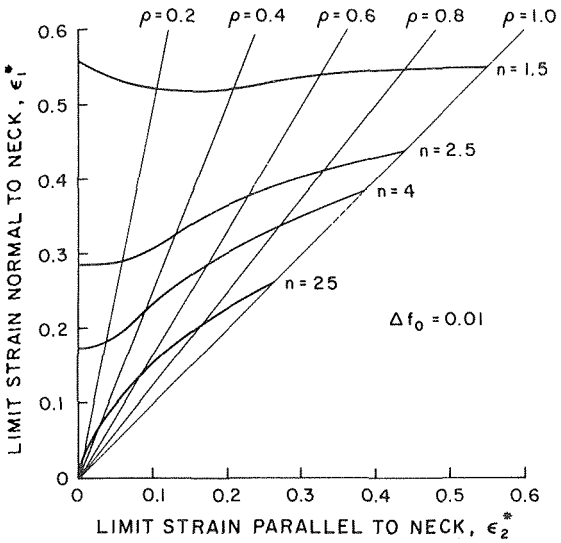


**Fig. 2 Predicted forming limit diagrams for various strain hardening exponents, $n^A = n^B = n$, with a difference between the initial void concentration inside the neck and that outside the neck, $\Delta f_o$, of 0.01**

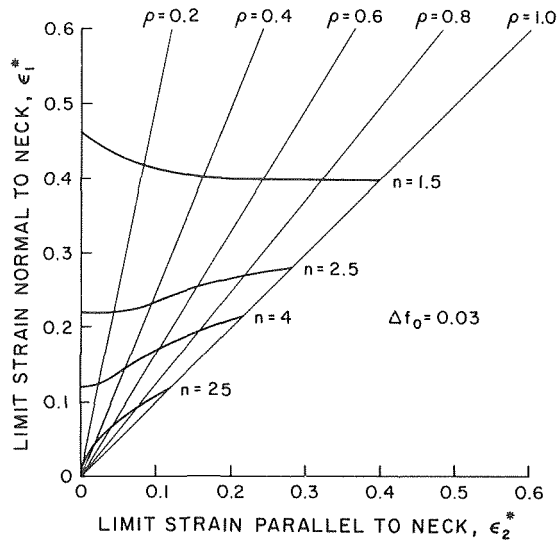


**Fig. 3 Predicted forming limit diagrams for various strain hardening exponents, $n^A = n^B = n$, with a difference between the initial void concentration inside the neck and that outside the neck, $\Delta f_o$, of 0.03**

of strain hardening exponents with real materials is only made for reference purposes. None of these materials is highly anisotropic ($r$-values range from 0.76 to 1.46) so that it is unlikely that any significant discrepancy between the experimental results and predictions based on a theory assuming isotropic material behavior can be attributed to anisotropy.

In Fig. 2, $\Delta f_0 = 0.01$, while in Fig. 3 $\Delta f_0 = 0.03$, where

$$\Delta f_0 \equiv f_0^B - f_0^A \tag{28}$$

The computations displayed in Figs. 2 and 3 were carried out with $f_0^A = 0$. Some were repeated with $f_0^A = 0.01$ and these results did not differ significantly from those displayed in the figures.

The most significant feature of the forming limit curves exhibited in Figs. 2 and 3 is that while for lightly or moderately hardening materials the limit strain, $\epsilon_1^*$, increases monotonically with imposed strain ratio, $\rho$, for a very high hardening material, $n = 1.5$, $\epsilon_1^*$ can initially decrease with $\rho$. For $n = 1.5$, with $\Delta f_0 = 0.01$, the limit strain $\epsilon_1^*$ reaches a minimum at about $\rho = 0.3$ and then increases again as $\rho$ approaches unity, while with $\Delta f_0 = 0.03$, $\epsilon_1^*$ is *nearly constant* for $\rho \geq 0.4$. For a somewhat lighter hardening material, $n = 2.5$, $\epsilon_1^*$ is nearly constant in the range $0 \leq \rho < 0.4$ with $\Delta f_0 = 0.03$, whereas when $\Delta f_0 = 0.01$ this range is narrowed to $0 \leq \rho < 0.2$.

This prediction of a relatively flat forming limit curve for high hardening materials with $d\epsilon_1^*/d\rho \leq 0$ at $\rho = 0$ is qualitatively in accord with the experimental observations in [5, 6] for stretched sheets. In the experiments, lightly hardening materials, with the exception of the results for Zircaloy reported in [5], tend to exhibit a rising forming limit curve. Zircaloy is a relatively lightly hardening material, $n \simeq 9$, for which $\epsilon_1^*$ is virtually independent of $\rho$. However, Zircaloy was also the only highly anisotropic material tested (an $r$-value of 4.54).

Quantitatively, the predicted forming limit curve are very sensitive to the assumed value of $\Delta f_0$. The values taken here, $\Delta f_0 = 0.01$ and $\Delta f_0 = 0.03$ give limit strains in the observed range but are probably unrealistically high for the materials of interest. This may be due to the fact that the constitutive equation employed [15, 16] uses a very simplified model of a voided material. The flow rule is derived by means of an analysis employing a perfectly plastic matrix. Workhardening is included in an approximate fashion. While the manner in which workhardening is included [15] is probably a reasonable approximation for lightly hardening materials, the degree to which the resulting flow rule models a high hardening material is certainly questionable. Furthermore, most voids present in the materials of interest in forming applications are probably nucleated during the deformation history, for example by inclusion cracking and/or debonding, rather than being initially present as assumed here. Nevertheless, even with due regard taken of the limitations of the constitutive model, the present results do clearly reveal the possibility that void growth may be responsible for the observed shapes of forming limit diagrams.

In Figs. 4 and 5, the forming limit curves resulting from various types of inhomogeneities are compared. The curves marked $(\sigma_y^B/\sigma_y^A) = 0.99$, correspond to a one percent yield stress reduction in region B, with all other initial values being identical in regions A and B. Similarly, the curves marked $(t^B/t^A)_0 = 0.99$, correspond to a one percent initial thickness reduction in region B with all other initial values being identical in regions A and B and so on. With the exception of the curves marked $\Delta f_0 = 0.01$, which, for comparison purposes are repeated form Fig. 2, the initial void concentrations in regions A and B was taken to be identically zero. With an initial void concentration of zero the constitutive equation described in Section 3 reduces to the Prandtl-Reuss equations and, therefore, the void concentration remains zero (excluding roundoff error) throughout the deformation history.

In Fig. 4, with $n^A = 1.5$, it is seen that the inhomogeneity corresponding to $(n^B/n^A) = 1.01$, gives qualitatively the same behavior as the model incorporating void growth. This is not entirely unexpected since the principle effect of void growth is to increasingly decrease the stiffness of the void matrix aggregate. On the other hand, the forming limit curves for $(\sigma_y^B/\sigma_y^A) = 0.99$ and $(t^B/t^A)_0 = 0.99$ monotonically increase with $\rho$.

In Fig. 5, with $n^A = 4$, all the forming limit curves have the same general shape, although the curve corresponding to $\Delta f_0 = 0.01$ is somewhat flatter.

These results have some bearing on the idea of an "equivalent thickness imperfection." In previous calculations of forming limit diagrams within the M-K [9] framework a thickness imperfection was employed as the inhomogeneity and it was hypothesized that this was representative of microstructural inhomogeneities. The present results show that this hypothesis is not necessarily appropriate for high hardening materials. However, in both Fig. 4 and Fig. 5 the curves with $(n^B/n^A) = 1.01$

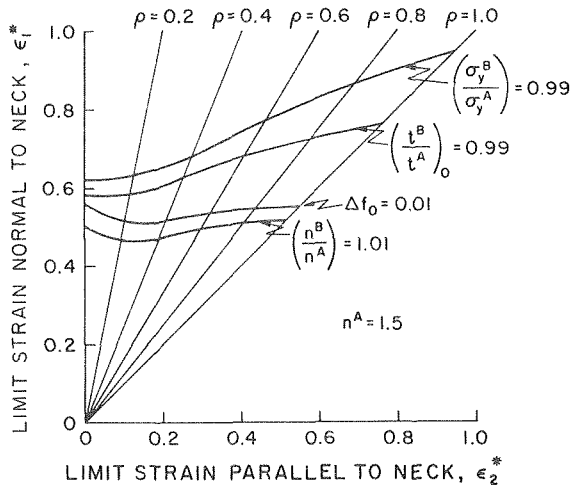


**Fig. 4 Comparison of the predicted forming limit diagrams resulting from various types of initial inhomogeneities with strain hardening exponent $n^A = 1.5$**

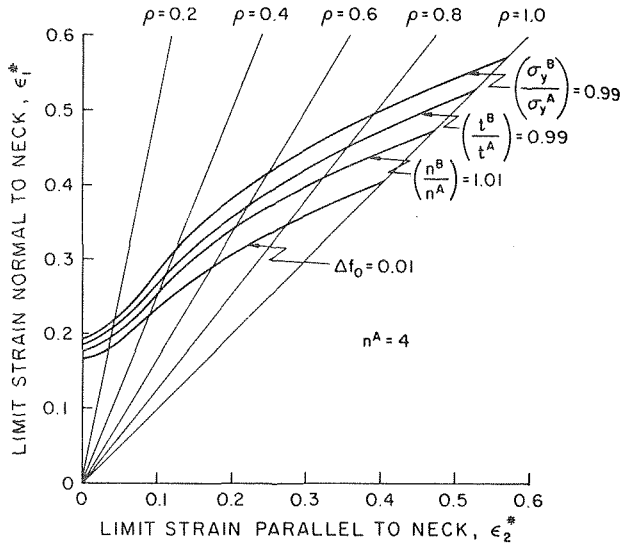


**Fig. 5 Comparison of the predicted forming limit diagrams resulting from various types of initial inhomogeneities with strain hardening exponent $n^A = 4$**

are qualitatively similar to those with $\Delta f_0 = 0.01$. Thus, any microstructural inhomogeneity that has the effect of continually decreasing the effective strain hardening exponent would be expected to give a qualitatively similar forming limit diagram. Although void growth is the most likely mechanism, it may not be the only possible one. In [5], Azrin and Backofen found no measureable effect of the inclusion content of copper on the forming limit diagram and, as mentioned previously, the most likely origin of voids is by inclusion cracking and/or debonding. However, voids could initially be present or nucleate by other means. Of course, it is also possible that void growth is not the mechanism responsible for triggering local necking in copper.

One notable feature of the computed deformation histories is that most of the void growth occurs just prior to the onset of local necking. As can be seen from (16), $f^B$ must approach unity when the limit strain is reached. However, with $n^A = n^B = 1.5$, $f_0{}^A = 0$, $f_0{}^B = 0.01$, the volume fraction of voids in the neck, $f^B$, at an imposed strain $\epsilon_1{}^A = 0.51$ varies from about 0.02 for $\rho$ near zero to 0.05 for $\rho = 1$. A similar variation of the volume fraction of voids in the neck, $f^B$, with imposed strain ratio, $\rho$, occurs with $n^A = n^B = 4$, $f_0{}^A = 0$, $f_0{}^B = 0.01$, at strains, $\epsilon_1{}^A$, slightly less than the limit strain.

## 5 Conclusions

The results of the present analysis indicate that the weakening effect of void growth could account for the observed shapes of forming limit diagrams. Since other physical mechanisms which result in such a weakening effect would be expected to predict qualitatively similar forming limit diagrams, no definite identification of void growth as the underlying physical mechanism can be made. In principle, this question could be resolved by experiment.

A more quantitative assessment of the influence of void growth on local necking might require a more realistic model of void growth in a high hardening matrix material. Furthermore, the effects of void nucleation need to be investigated. Although the limitations inherent in the constitutive equation employed in this investigation are recognized, the results obtained using it are regarded as being encouraging regarding the utilization of constitutive equations incorporating microstructural features in the analyses of sheet metal forming problems.

The bifurcation analysis of Stören and Rice [14], based on a simple model of a material with a vertex on its yield surface, also predicts forming limit diagrams qualitatively in accord with experiment, although differing somewhat in detail from the ones obtained here. Both vertex effects and void growth or other microstructural inhomogeneities may contribute to determining the observed shape of forming limit diagrams and the relative importance of these effects could vary from material to material.

## Acknowledgment

The support of this work by the NSF through Grant ENG76-16421 is gratefully acknowledged.

## References

1 Hill, R., "On Discontinuous Plastic States, with Special Reference to Localized Necking in Thin Sheets," *Journal of the Mechanics and Physics of Solids*, Vol. 1, 1952, pp. 19–30.

2 Keeler, S. P., "Understanding Sheet Metal Formability," *Machinery*, Vol. 74, Nos. 6–11, Feb.–July 1968.

3 Hecker, S. S., "Simple Technique for Determining Forming Limit Curves," *Sheet Metal Industries*, 1975, pp. 671–675.

4 Hecker, S. S., "Formability of Aluminum Alloy Sheets," ASME JOURNAL OF ENGINEERING MATERIALS AND TECHNOLOGY, Vol. 97, 1975, pp. 66–73.

5 Azrin, M., and Backofen, W. A., "The Deformation and Failure of a Biaxially Stretched Sheet," *Metallurgical Transactions*, Vol. 1, 1970, pp. 2857–2865.

6 Ghosh, A. K., and Hecker, S. S., "Stretching Limits in Sheet Metals: In-Plane Versus Out-of-Plane Deformation," *Metallurgical Transactions*, Vol. 5, 1974, pp. 2161–2164.

7 Ghosh, A. K., and Hecker, S. S., "Failure in Thin Sheets Stretched over Rigid Punches," *Metallurgical Transactions*, Vol. 6A, 1975, pp. 1065–1074.

8 Painter, M. J., and Pearce, R., "Instability and Fracture in Sheet Metal," *Journal of Physics D: Applied Physics*, Vol. 7, 1974, pp. 992–1002.

9 Marciniak, A., and Kuczynski, K., "Limit Strains in the Process of Stretch Forming Sheet Metal," *International Journal of the Mechanical Sciences*, Vol. 9, 1967, pp. 609–620.

10 Sowerby, R., and Duncan, J. L., "Failure in Sheet Metal in Biaxial Tension," *International Journal of the Mechanial Sciences*, Vol. 13, 1971, pp. 217–229.

11 Marciniak, A., Kuczynski, K., and Pokora, T., "Influence of the Plastic Properties of a Material on the Forming Limit Diagram for Sheet Metal in Tension," *International Journal of the Mechanical Sciences*, Vol. 15, 1973, pp. 789–805.

12 van Minh, H., Sowerby, R., and Duncan, J. L., "Probabilistic Model of Limit Strains in Sheet Metal," *International Journal of the Mechanical Sciences*, Vol. 17, 1975, pp. 339–349.

13 Needleman, A., "Necking of Pressurized Spherical Membranes," *Journal of the Mechanics and Physics of Solids*, Vol. 24, 1976, pp. 339–359.

14 Stören, S., and Rice, J. R., "Localized Necking in Thin Sheets," *Journal of the Mechanics and Physics of Solids*, Vol. 23, 1975, pp. 421–441.

15 Gurson, A. L., "Plastic Flow and Fracture Behavior of

Ductile Materials Incorporating Void Nucleation, Growth and Interaction," PhD thesis, Brown Univ., 1975 (available from University Microfilms, Ann Arbor, Mich.).

16 Gurson, A. L., "Continuum Theory of Ductile Rupture by Void Nucleation and Growth: Part I—Yield Criteria and Flow Rules for Porous Ductile Materials," ASME JOURNAL OF ENGINEERING MATERIALS AND TECHNOLOGY, Vol. 99, 1977, pp. 2–15.

17 Yamamoto, H., "Conditions for Shear Localization in the Ductile Fracture of Void Containing Materials," Brown University Report E(11-1) 3084/50, Apr. 1977.

18 Rice, J. R., "The Localization of Plastic Deformation," *Proceedings of the 14th International Congress and Theoretical and Applied Mechanics*, (Delft, August 30 – September 4, 1976) (edited by Koiter, W. T.), Vol. 1, North-Holland, Amsterdam, 1976, pp. 207–220.

19 Berg, C. A., "Plastic Dilation and Void Interaction," in *Inelastic Behavior of Solids*, eds. M. F. Kanninen, et al., McGraw-Hill, 1970, pp. 171–209.

20 Bishop, J. F. W., and Hill, R., "A Theory of the Plastic Distortion of a Polycrystalline Aggregate Under Combined Stress," *Philosophical Magazine*, Vol. 42, 1951, pp. 414–427.